68. Coenzyme F430 from Methanogenic Bacteria: Complete Assignment of Configuration Based on an X-Ray Analysis of 12,13-Diepi-F430 Pentamethyl Ester and on NMR Spectroscopy

by **Gerald Färber, Walter Keller,** and **Christoph Kratky***

Institut für Physikalische Chemie, Universität Graz, Heinrichstrasse 28, A–8010 Graz

and **Bernhard Jaun***, **Andreas Pfaltz**[1])*, **Christoph Spinner, André Kobelt,** and **Albert Eschenmoser**

Laboratorium für Organische Chemie, Eidgenössische Technische Hochschule, Universitätstrasse 16, CH–8092 Zürich

(4.II.91)

The structure of a derivative of coenzyme F430 from methanogenic bacteria, the bromide salt of 12,13-diepi-F430 pentamethyl ester (**5**, X = Br), was determined by X-ray structure analysis. It reveals a more pronounced saddle-shaped out-of-plane deformation of the macrocycle than any hydroporphinoid Ni complex investigated so far. The crystal structure confirms the constitution proposed for coenzyme F430 (**2**) and shows that in the epimer **5**, the three stereogenic centers in ring D, C(17), C(18), and C(19), have the (17*S*)-, (18*S*)-, and (19*R*)-configuration, respectively. Deuteration and 2D-NMR studies independently demonstrate that native coenzyme F430 (**2**) has the same configuration in ring D as the epimer **5**. Therefore, our original tentative assignment of configuration at C(19) and C(18) [1] has to be reversed. This completes the assignment of configuration for all stereogenic centers in coenzyme F430, which has the structure shown in *Formula* **2**.

1. Introduction. – In the previous papers in this series [1–4], we reported on the structure elucidation of coenzyme F430 [5] [6], a hydroporphinoid nickel complex which plays a central role in the energy metabolism of methanogenic bacteria [7]. As a component of methyl-coenzyme M reductase, it catalyzes the reductive cleavage of *S*-methyl-coenzyme M to coenzyme M and methane [8] [9].

Our structural studies which were carried out in close collaboration with the group of *R. K. Thauer* at the University of Marburg led to the structural formula **1** for coenzyme F430 (R = H). The constitution was determined largely by NMR analysis of the pentamethyl ester F430M in combination with a series of biosynthetic incorporation experiments using specifically ^{13}C-labeled precursors [1a] and UV/VIS studies of synthetic hydrocorphinoid model complexes [1b]. Making extensive use of 1D-NOE-difference spectroscopy, it was possible to establish the relative configuration at the six stereogenic centers in rings A and B and the *trans*-arrangement of the ring-C side chains, but not the configurational relationship between rings B and C. The absolute configuration at C(12) and C(13) was deduced by ozonolytic excision of ring C and CD-spectroscopic correlation of the resulting succinimide derivative with reference compounds of known absolute configuration [1a]. The absolute configuration of the A/B fragment followed from comparison of the CD spectra of nickel(II) isobacteriochlorinate derivatives prepared from F430 with the CD spectrum of nickel(II) sirohydrochlorinate octamethyl ester [4].

[1]) Present address: Institut für Organische Chemie, Universität Basel, St. Johannsring 19, CH–4056 Basel.

In ring D, the configuration at the stereogenic centers C(17), C(18), and C(19) could not be established unambiguously. Interpretation of observed NOE's based on model considerations and use of chemical-shift arguments led to tentative assignments for C(18) and C(19) as shown in *Formula* **1**, whereas the configuration at C(17) remained unassigned.

Subsequently, considerable efforts were made to crystallize F430 and F430M, but the crystals obtained so far were unsuitable for X-ray structure analysis. However, preliminary results from an X-ray analysis of 12,13-diepi-F430M, the pentamethyl ester of an isomer produced by thermal isomerization of F430 [3], indicated that the absolute configuration at C(19) was *not* (19*S*) but (19*R*), with an all-*trans*-arrangement of H–C(17), H–C(18), and H–C(19) [10]. Unfortunately, this crystal structure showed several regions of disorder, one of them about C(18), and did not allow unequivocal configurational assignments in ring D. Therefore, NMR studies including 2D-NMR spectroscopy of F430 derivatives were resumed. Further crystallization experiments with 12,13-diepi-F430M eventually led to crystals which, although they were still partially disordered, allowed an unambiguous assignment of configuration in ring D by X-ray structure determination. At the same time, this crystal-structure analysis yielded the first atomic resolution image of a molecule closely related to coenzyme F430.

In the following, we discuss the results of this analysis which conclusively shows that 12,13-diepi-F430M has the (17*S*,18*S*,19*R*)-configuration. Furthermore, we show by deuteration experiments and NMR studies that 12,13-diepi-F430M and the parent coenzyme F430 have the same configuration in ring D. *This implies that our original tentative assignment of configuration at centers C(18) and C(19)* [1] *must be reversed and that the absolute configuration of coenzyme F430 in ring D is (17*S*,18*S*,19*R*) as shown in* Formula **2**.

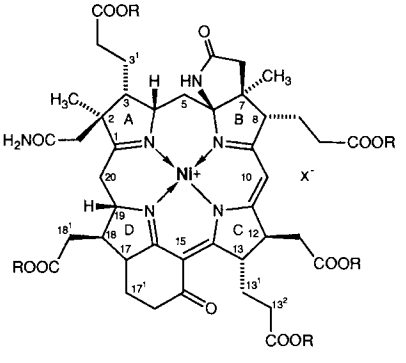

1 R = H; coenzyme F430
original tentative assignment of configuration
incorrect at C(18) and C(19) [1]

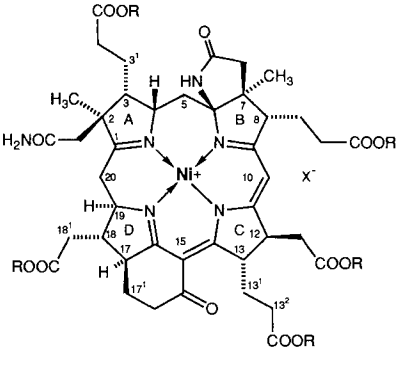

2 R = H; coenzyme F430
revised assignment

Recently, *Summers* and coworkers published an investigation of the solution structure of coenzyme F430, using various 2D-NMR methods and distance-geometry computations combined with back-calculations of NOESY spectra [11]. Their results confirmed the constitution of F430 as well as our previous configurational assignments in rings A, B, and C. Their data also indicated an all-*trans*-arrangement of H–C(17), H–C(18),

and H–C(19), but did not allow to distinguish between the (17*S*,18*S*,19*R*)- and (17*R*,18*R*,19*S*)-configuration.

2. Crystal Structure of 12,13-Diepi-F430M (**5**, X = Br). – Among the various F430 derivatives investigated so far, only the bromide salt 12,13-diepi-F430M (**5**, X = Br) formed crystals of suitable quality for an X-ray analysis. The corresponding chloride, perchlorate, acetate, and thiocyanate salts yielded only microcrystalline or amorphous solids. The parent 12,13-diepi-F430 (**4**) was obtained when a degassed aqueous solution of coenzyme F430 (**2**) at pH 7–8 was heated for several h to 100°. This led to an equilibrium mixture, consisting largely of **4** (88%), 13-epi-F430 (8%), and **2** (4%) [3]. From this mixture, analytically pure 12,13-diepi-F430M (**5**, X = ClO_4) could be prepared by methanolysis (CH_3OH, TsOH, 50°) followed by prep. TLC on $NaClO_4$-coated silica-gel plates.

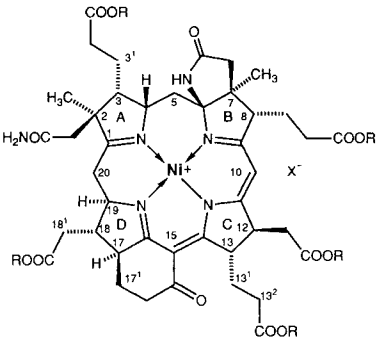

2 R = H; coenzyme F430
3 R = CH_3, X = ClO_4; F430M

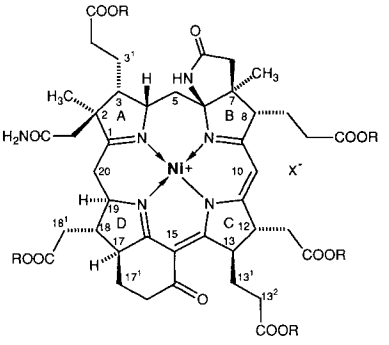

4 R = H; 12,13-diepi-F430
5 R = CH_3, X = ClO_4 or Br; 12,13-diepi-F430M

For the X-ray analysis, a sample of perchlorate **5** (X = ClO_4), which had been characterized by ^{1}H-NMR spectroscopy (see *Chapt. 4*) and shown to be analytically pure was converted to the corresponding bromide **5** (X = Br)[2]). From a super-saturated solution of the bromide **5** in AcOMe/CH_2Cl_2 10:1, reddish-brown crystals were obtained upon standing at room temperature for several days.

The crystal-structure analysis drew on experience from a previous analysis [10] of a crystal obtained under similar crystallization conditions. This analysis had suffered from severe disorder, precluding an indisputable assignment of the ring-D configuration. At that time, the possibility could not be excluded that the disorder might be due to the incorporation of a second stereoisomer into the crystal or to an incorrect assignment of the space group (*P*1 instead of *R*3). In the present analysis, both possibilities were considered but, eventually, could be ruled out (see *Exper. Part*).

Disorder also affected the present crystal-structure analysis, but thanks to a number of experimental precautions (collection of a very comprehensive set of reflection data at

[2]) Due to coordination of the bromide to the Ni^{II} ion, solutions of 12,13-diepi-F430 M (**5**, X = Br) are slightly paramagnetic. This leads to considerable line-broadening in the ^{1}H-NMR spectrum. Therefore, all NMR experiments with **5** were carried out using the perchlorate rather than the bromide salt.

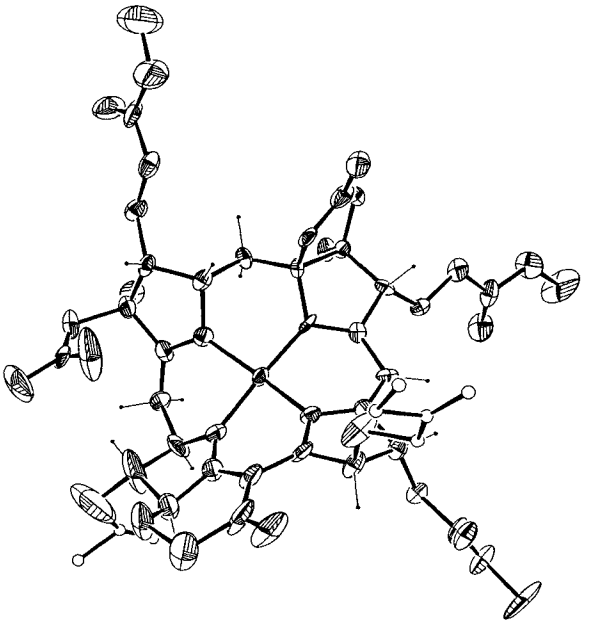

Fig. 1. *ORTEP drawing of the 12,13-diepi-F430M* (**5**, X = Br) *molecule from the crystal structure.* Ellipsoids are drawn at the 50% probability level. Only the conformation with the higher occupancy is shown for the disordered side chains at C(13) and C(18); the corresponding atoms are represented as spheres with arbitrary radius. H-Atoms are omitted, with the exception of those directly attached to the porphinoid ring which are represented as small spheres.

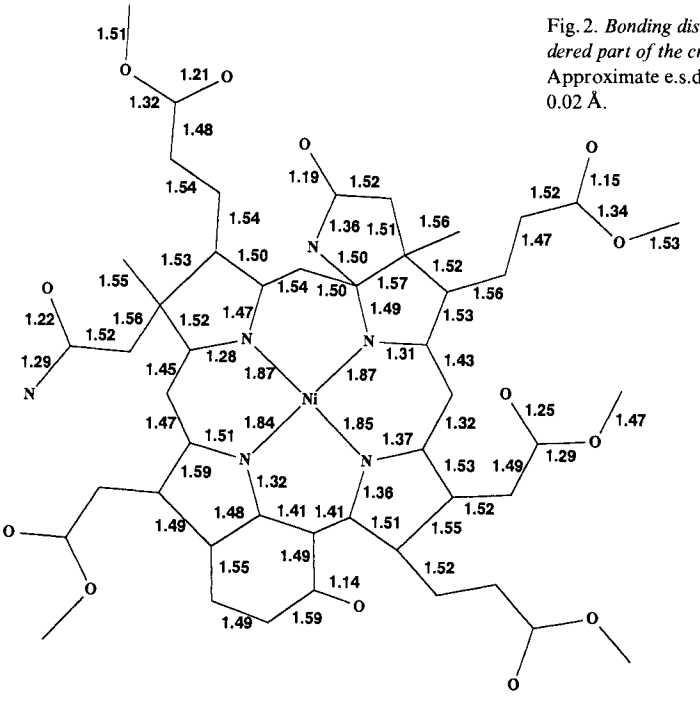

Fig. 2. *Bonding distances* [Å] *for the non-disordered part of the crystal structure of* **5** (X = Br). Approximate e.s.d. of the bonding distances 0.02 Å.

low temperature from a large, carefully chosen crystal specimen of low mosaicity), it was possible to interpret the electron density with a model involving alternatively occupied atomic sites for most of the disordered regions. This led to a reasonably accurate structure analysis, which also involved a determination of the absolute configuration from the anomalous contribution of the Br^- counter ion.

The 12,13-diepi-F430M (**5**, X = Br) crystallizes in the rhombohedral space group $R3$ with nine molecules per unit cell (hexagonal setting). The structure analysis was based on intensity data collected at 93 K for a full hemisphere of reciprocal space to $\sin\theta/\lambda = 0.59$ $Å^{-1}$. The refinement converged at $R = 0.0787$ and $R_w = 0.061$ for 677 parameters and 3927 unique observations. A computer-drawing of the 12,13-diepi-F430M molecule is shown in *Fig. 1*, the numbering system used for the description of the structure is defined in *Formula* **5**, and a selection of observed bond lengths is given in *Fig. 2*. *Fig. 3* shows a stereoscopic packing diagram of three molecules related by the operation of the threefold axis.

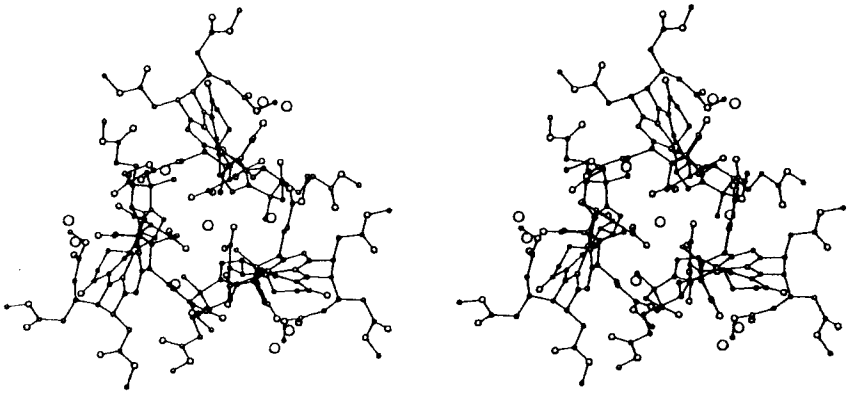

Fig. 3. *Stereoscopic packing diagram of the crystal structure of* **5** (X = Br). Projection along the threefold axis.

Disorder. Disorder was observed in the following regions: *i*) The bromide anion was found to be distributed over four positions: one of them is located at the threefold axis (multiplicity 1/3, fully occupied), the other three lie on general positions (multiplicity 1) and were observed to be partially occupied. All four positions were refined with anisotropic atomic-displacement parameters (a.d.p.'s); for the three general positions, the site-occupation factor was also allowed to refine. At the close of the refinement, the sum of the products of the four s.o.f.'s with their corresponding multiplicities added up to 0.987(21), supporting the conclusion that most of the Br^- electron density had been accounted for.

ii) The propionate side chain at C(13) was observed in two conformations, differing in the positions of C(13^2) and the COOMe group. Both conformations were included in the refinement, a common s.o.f. was refined for each conformation, subject to the constraint that the sum of the two s.o.f.'s adds up to unity. One of the two conformations (s.o.f. 0.33) shows the propionate chain folded above the macrocyclic ring plane, placing the carbonyl O-atom of the COOMe group above the Ni center, at a distance of *ca.* 3.5 Å. This position is very close to two partially occupied Br^- positions, which thus appear to compete for the

axial coordination site of the Ni center. The other conformation (s.o.f. 0.67) extends away from the macrocycle, into the region of the (also disordered) C(18) acetate side chain of a symmetry-equivalent molecule.

iii) The ester group of the C(18) acetate side chain was also found in two conformations, which were treated similarly to the C(13) substituent. The s.o.f.'s of the two conformations converged to 0.77 and 0.23, the MeO C-atom of COOMe could not be located for either of the two conformations.

iv) A disordered and partially occupied (s.o.f. 0.65) solvent molecule, probably a molecule of AcOMe was located near the position of the C(13) propionate side chain in its more populated conformation.

The Placement of C(18) and Its Substituent. The preceding structure analysis [10] had encountered difficulties in the refinement of the C(18) atom, the position of which is crucial for the configurational assignment of the three asymmetric ring-D atoms. Although this atom behaved well in the present refinement (no non-positive-definite atomic-displacement ellipsoids), we carried out the following test: the structure was refined with individual isotropic a.d.p.'s, omitting the C(18) atom, all the atoms of the acetate side chain attached to C(18), the disordered atoms of the C(13) ester side chain, the disordered solvent molecule, and all H-atoms. This refinement converged at $R = 0.147$, $R_w = 0.133$.

A difference electron-density map was subsequently computed, and sections perpendicular to the line connecting the atoms C(17) and C(19) were contoured. Irrespective of

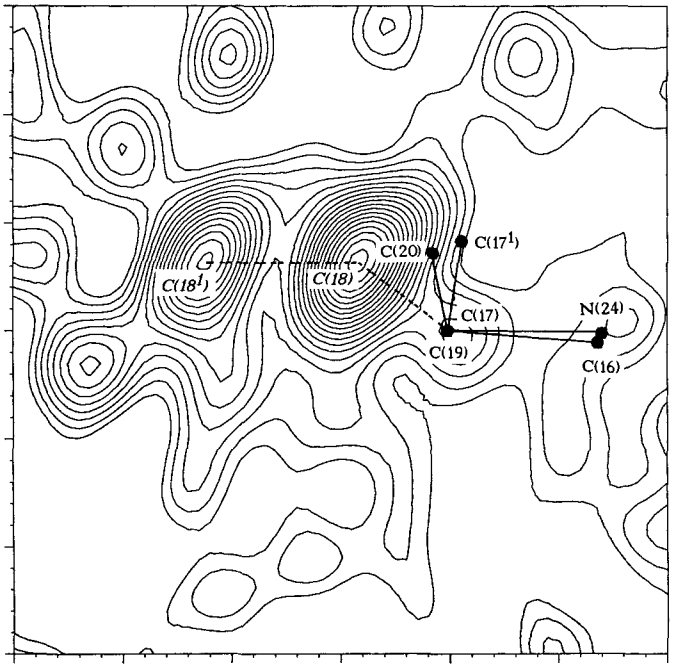

Fig. 4. *Difference electron-density map locating C(18) and its substituent.* Section perpendicular to and bisecting the line C(17)–C(19). Only positive electron density was contoured. Lowest contour line at 0.1 eÅ^{-3}, increment between successive contour lines 0.1 eÅ^{-3}.

the ring-D conformation, C(18) and the first atom of the acetate side chain, C(18^1), should both lie in the plane (shown in *Fig. 4*) bisecting the distance between C(17) and C(19), as long as C(17) and C(19) are not disordered (which they are not). The difference electron density map shows conclusively that C(18) and C(18^1) are both well defined and that H–C(18) points towards the β-face of the corphinoid ring ('upwards' in *Fig. 4*).

The Conformation of the Hydrocorphinoid Ring System of **5** *in the Crystal.* Through a series of crystal-structure analyses of hydroporphinoid model compounds, we have established earlier [12a] that the dominant response to the contraction of the central N_4-coordination hole, necessary to optimally accomodate 'small' metal centers (such as diamagnetic Ni^{II}), is a *saddle-shaped conformation of the hydroporphinoid ring*. This saddle conformation manifests itself in a characteristic wave-shaped cylinder projection, as shown in *Fig. 5a* for nickel(II) *ccccc*-octaethylpyrrocorphinate (*c* = *cis*, starting from ring

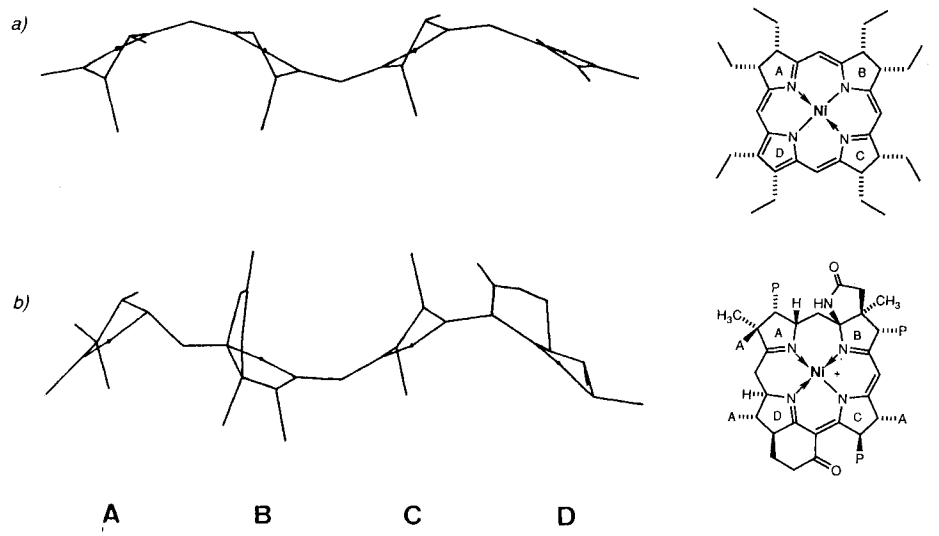

Fig. 5. *Cylinder projections* (cylinder radius 2.5 Å) *of* a) *nickel(II)* ccccc-*octaethylpyrrocorphinate* (from [1]) *and* b) *12,13-diepi-F430M* (**5**; X = Br). Only the first C-atom of each noncyclic side chain has been drawn.

A and proceeding to rings B–D). As a quantitative measure for the degree of saddle deformation, we introduced the mean absolute deviation of the four *meso*-C-atoms from a least-squares plane through the four pyrrolic N-atoms ($d_m = [|d(C(5))| + |d(C(10))| + |d(C(15))| + |d(C(20))|]/4$)[3]. The largest d_m value was so far observed for the nickel(II) *ccccc*-octaethylpyrrocorphinate shown in *Fig. 5a* ($d_m = 0.75$ Å [12a]).

According to our analysis, the inherent size of the N_4 cavity increases with increasing degree of saturation of the porphinoid ring, and so does the flexibility of the macrocyclic

[3]) This definition of the d_m value yields an unrealistic measure for the degree of saddle deformation when the porphyrin ring contains saturated C-atoms [12a]. In such cases, we compute d_m from the corresponding non-planarities of an analytical saddle plane obtained by a least-squares fit to the atoms of the macrocyclic ring [12b]. The value of $d_m = 1.04$ Å quoted for **5** was calculated in this way; from the perpendicular displacements of the four *meso* C-atoms, a value of $d_m = 0.78$ Å is obtained for **5**.

ring [12a]. For a given metal atom, both factors cooperatively work towards an increase in saddle deformation with increasing number of hydrogenated double bonds. Accordingly, a large saddle deformation was to be expected for F430 with low-spin Ni^{II} [3].

The information collected in *Figs. 2, 5,* and *6* indeed shows that **5** assumes a highly ruffled, saddle-shaped conformation with short equatorial Ni–N bonds ($\langle d(Ni–N)\rangle = 1.86$ Å). The degree of saddle deformation ($d_m = 1.04$ Å)[4]) is even larger than for nickel(II) *cccc*-octaethylpyrrocorphinate ($d_m = 0.75$ Å). Thus, **5** shows the largest saddle deformation observed so far for a hydroporphinoid metal complex. The N_4 coordination is slightly distorted from planarity towards a tetrahedral N_4 arrangement, as seen from the alternating deviations of the pyrrolic N-atoms by *ca.* 0.2 Å above and below the mean plane.

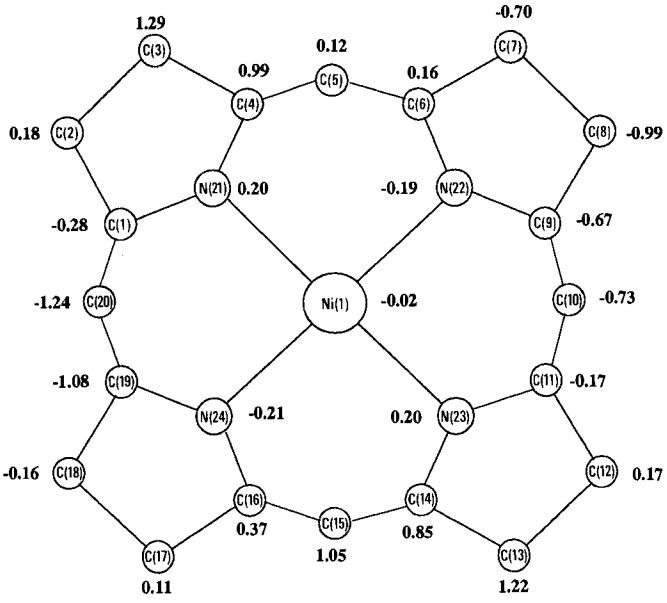

Fig. 6. *Perpendicular deviations of the macrocyclic ring atoms from a least-squares plane through the atoms N(21), N(22), N(23), and N(24) for the crystal structure of* **5** (X = Br)

Conformation of Rings A and C. Compared to native F430, the 12,13-diepi-F430 is thermodynamically more stable and shows a lower tendency towards conversion into the high-spin form [3]. Both observations have been interpreted in terms of a structural property particular to hydroporphinoid low-spin Ni^{II} complexes, namely the *conformational coupling* of the hydropyrrolic rings [12a]: the overall saddle conformation induced by the adaption of the hydroporphinoid ring to the stereochemical requirement of 'small' metal centers enforces a 'wave-shaped' alternation of the half-chair conformation of the hydropyrrolic rings (W-conformation). The resulting characteristic features of the cylinder projection and its schematic abstraction are shown in *Fig. 7a.*

---

[4]) The large saddle deformation contradicts theoretical results based on a combination of monte carlo and molecular mechanics calculations [13], which predict an almost flat ($d_m < 0.28$ Å) minimum energy structure for F430 with a Ni–N distance of 1.85 Å.

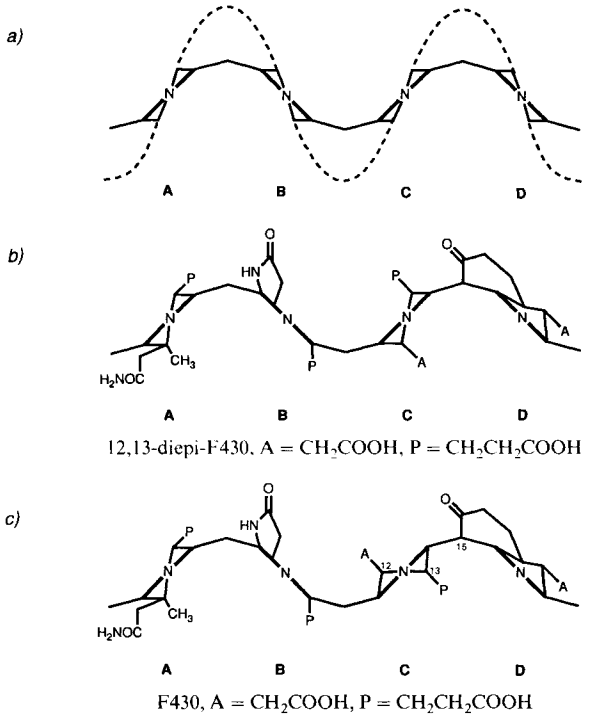

Fig. 7. a) *Schematic representation of the conformational coupling of nickel(II) hydrocorphinates* (the preferred W-conformation), b) *12,13-diepi-F430, and* c) *F430; structural rationalization of the higher thermodynamic stability of 12,13-diepi-F430 as opposed to F430.* In F430, the quasi-axial position of the C(13) substituent enforced by steric interaction with the carbonyl group attached to C(15) results in the 'wrong' half-chair conformation for ring C (from [3]).

NMR evidence and model considerations indicate that the Me group attached to ring A and the two substituents at ring C are in a quasi-axial conformation for both, F430M (**3**) [1] and 12,13-diepi-F430M (**5**) [3]. As illustrated in *Fig. 7*, this led to the conclusion that the half-chair conformations of rings A and C conform to the (energetically preferred) W-conformation in 12,13-diepi-F430, *but not in native F430* [3]. The crystal structure of **5** (*Fig. 5b*) indeed shows the predicted conformations for rings A and C, which supports the arguments given in [3][5]). A more detailed discussion would require a crystal structure of a F430 derivative with the native ring-C configuration, for which we expect a more strained macrocyclic ring with a smaller d_m.

3. Configuration of Coenzyme F430. – In order to resolve the remaining ambiguities in the configurational assignments of coenzyme F430 (**2**), we needed a rigorous stereochemical correlation between **2** and the F430 derivative **5**, the relative and absolute configuration of which was established by crystal-structure analysis. We had previously shown that

[5]) In contrast to rings A and C which are conformationally flexible, rings B and D are conformationally locked. Therefore, they cannot assume regular half-chair conformations conforming to the usually preferred W-arrangement.

under the conditions used for converting the pentaacids **2** and **4** to the pentamethyl esters **3** and **5**, no epimerization occurred [3]. Our original conclusion that the two isomers **2** and **4** differ solely in their configuration at C(12) and C(13) was based on the NMR data of the corresponding pentamethyl esters **3** and **5** (and with respect to ring D, on chemical reasoning) [3]. Further evidence for this assumption came from the observation that 12,13-didehydro-F430, formed from F430 (**2**) by dehydrogenation with O_2, could be reduced with Zn/AcOH to a mixture of F430 (**2**) and the same two isomers which had been previously obtained by thermal isomerization of **2** and which had been identified as 13-epi-F430 and 12,13-diepi-F430 (**4**) [3]. A proof that the thermal epimerization of F430 (**2**) involved only C(12) and C(13) in ring C, while all other stereogenic centers retained their configuration, was finally obtained by the deuterium-incorporation studies summarized in *Scheme 1*.

Scheme 1

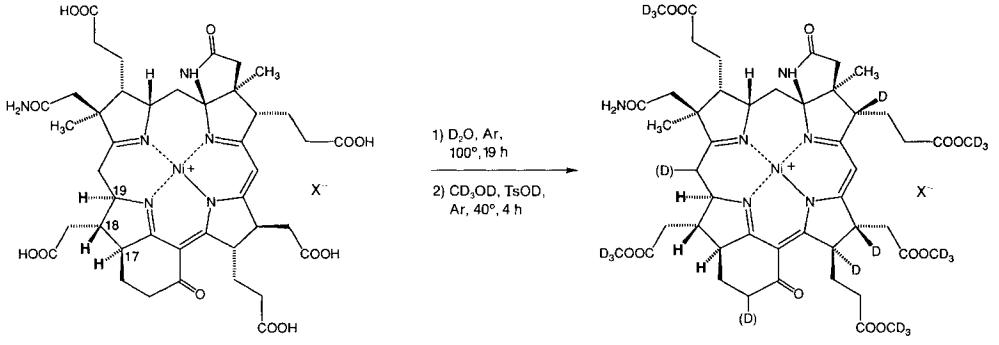

2 F430 [D]-**5**, 12, 13-diepi-[D]F430M

Coenzyme F430 (**2**) was epimerized in D_2O under the usual conditions at 100° under Ar [3]. After lyophilization of the reaction mixture, the residue was taken up in CD_3OD and, after addition of TsOD, heated to 40° for 4 h (formation of the penta[D_3]methyl-ester). Aqueous workup and prep. TLC on $NaClO_4$-coated silica-gel plates afforded polydeuterated [D]-**5** as the main product in *ca.* 40% yield. According to the ^{1}H-NMR[6]) spectrum, no D was incorporated at C(19), whereas C(8), C(12), and C(13) were fully and C(20) partially substituted with D[7]). The remaining deuterated positions were identified by ^{13}C-NMR spectroscopy. All signals of deuterated C-atoms (C(8), C(12), C(13), C(17^2), and C(20)) were suppressed in the ^{1}H-broad-band decoupled ^{13}C-NMR spectrum (due to their long relaxation time, smaller NOE, and splitting by ^1J(C,D)). In contrast, the signals of C(17), C(18), and C(19) were present at their natural intensity within experimental error, confirming that no significant amount of D was incorporated at these centers. Hence, F430M (**3**) must have the same configuration at C(17) and C(18) as the stereoisomers **5**, the structure of which is based on X-ray analysis.

---

[6]) ^{2}H-NMR spectroscopy did confirm deuterium incorporation at several positions, but in the region of severe spectral overlap (3.0–1.5 ppm), large line-widths (*ca.* 100 Hz) precluded assignment to individual sites.

[7]) The amide and lactam N-atoms which must become deuterated under the reaction conditions presumably underwent D/H exchange during workup and purification by TLC.

Scheme 2

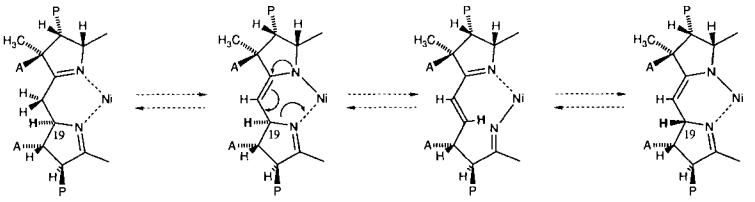

A = CH_2COR, P = CH_2CH_2COR

In contrast to C(17) and C(18), the deuteration experiments do not allow a definite assignment for C(19) because, in principle, it is possible to formulate a mechanism for inverting its configuration without H/D exchange (*Scheme 2*). Since C(17) does not epimerize during the thermal conversion of **2** into **4**, epimerization at C(19) *via* the mechanism of *Scheme 2* would imply a *trans*-arrangement of H–C(17) and H–C(19) in coenzyme F430 (**2**). However, the ^{1}H-NMR data of F430M (**3**) discussed in *Chapt. 4* (for F430, see [11]), clearly show that H–C(17) and H–C(19) are *cis* to each other. Accordingly, coenzyme F430 (**2**) must have the same configuration at C(17), C(18), and C(19) as the epimerization product **4**.

4. NMR Spectroscopy of F430M (3) and 12,13-Diepi-F430M (5, X = ClO_4). – Correlation of the configuration at C(19) with the known configuration at C(2) by means of NMR spectroscopy critically depends on the observation of nuclear *Overhauser* effects (NOE) between protons attached to substituents at C(2) and the nonequivalent CH_2(20) protons on one hand, and between CH_2(20) and H–C(19), H–C(18) and/or CH_2(18^1) on the other hand. Under conditions giving well resolved, fully diamagnetic spectra (dry CD_2Cl_2, 25°), the correlation times of both F430M (**3**) and 12,13-diepi-F430M (**5**, X = ClO_4) were such, that only very small, positive NOE's were observed (0.05–2%). Using 1D-NOE-difference spectroscopy of **3** under these conditions, roughly comparable NOE's were observed between CH_3–C(2) and each of the two CH_2(20) protons [1]. However, all attempts to detect NOE's between the latter and H–C(19) failed because strong SPT effects [14], arising from scalar coupling between these three protons, completely obscured possible NOE responses. As expected, cross-peak intensities in NOESY spectra [15] (CD_2Cl_2, 25°) were too weak to yield interpretable data. ROESY spectra [16] did confirm all NOE's between non-coupled protons observed earlier, but the crucial cross-peaks between H–C(19), H–C(20), and H′–C(20) were dominated by strong antiphase signals due to scalar coupling [16b].

At lower temperatures (–10 to –25°, CD_2Cl_2), the correlation time of **3** proved to be long enough to make moderately strong negative NOE's observable. However, with decreasing temperature, the line-width increased to a much larger extent than expected from the increase in viscosity of the solvent, making assignments of individual protons difficult[8]). Using $CDCl_3$ as solvent, an optimized temperature (*ca.* 0°) could eventually be found, at which NOE's were negative while the lines remained sufficiently sharp to

[8]) The broadening and chemcial-shift variation of specific signals observed upon decreasing the temperature indicate an increase of the fraction of F430 M (**3**) present in the paramagnetic five- or six-coordinate forms at lower temperature. This is confirmed by the fact that 12,13-diepi-F430 M (**5**, X = ClO_4), which has a much lower tendency to coordinate additional ligands axially, shows well resolved spectra even at –10°.

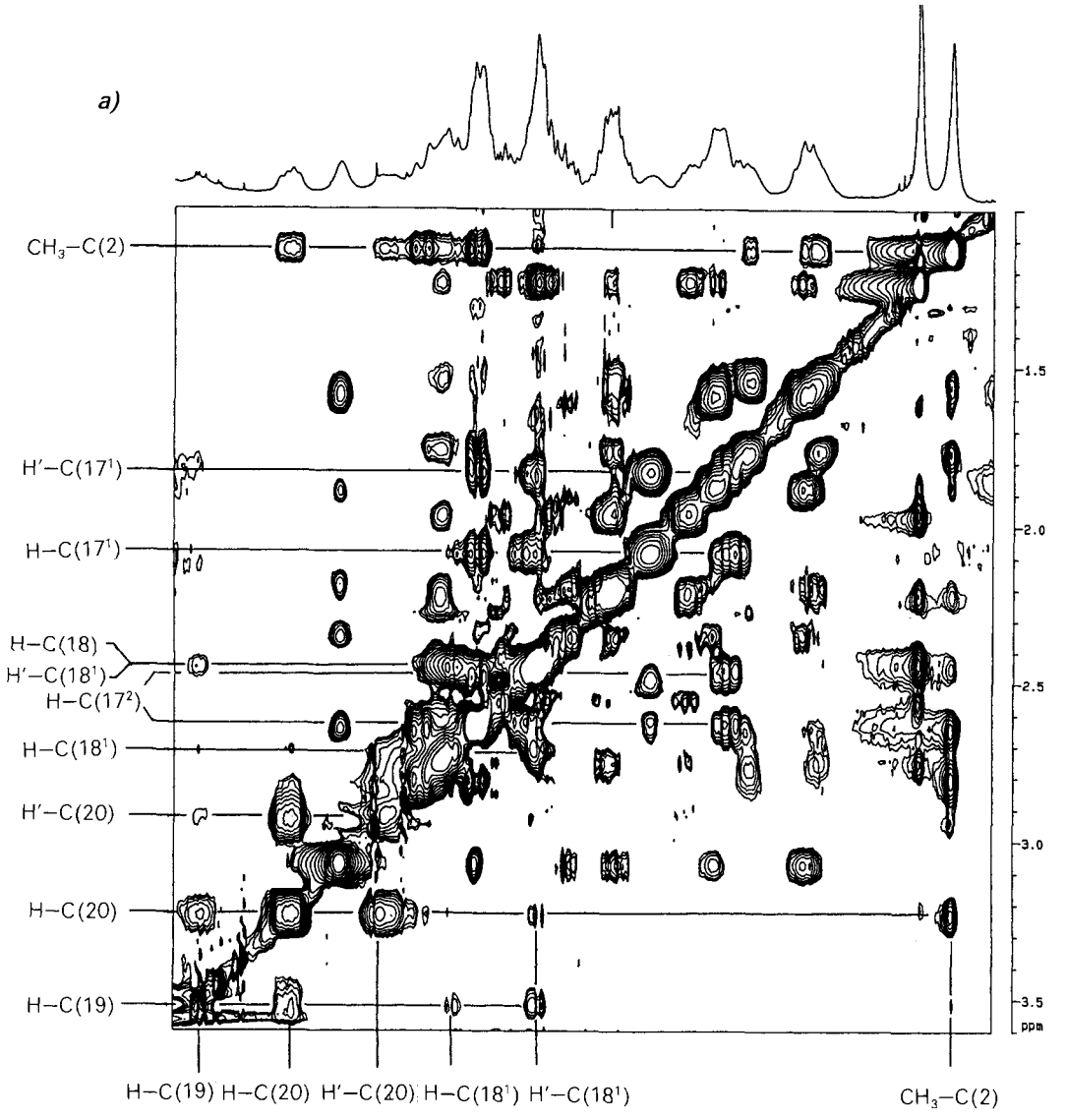

Fig. 8. *NOESY spectra of* a) *F430M* (**3**) *and* b) *12,13-diepi-F430M* (**5**, X = ClO_4) *in* $CDCl_3$ *at 0°*. Mixing time 240 ms (for other parameters, see *Exper. Part*). The labeled protons were assigned by TOCSY at 0° in $CDCl_3$. In some cases, the order and value of their chemical shifts differ significantly from those at 25° in CD_2Cl_2 which are reported in *Tables 1* and *2*.

identify all proton signals of **3** by TOCSY [17], HMQC [18], and comparison with the well resolved 2D-NMR spectra obtained in CD_2Cl_2 at 25°[9]). For **5** (X = ClO_4), the sign and intensities of NOE's at different temperatures in CD_2Cl_2 and $CDCl_3$ closely paralleled those of **3** but the line-width increased only slightly at low temperature. NOESY spectra

[9]) The signals of all protons and all proton-bearing C-atoms of both **3** and **5** were assigned as shown in *Tables 1* and *2* based on COSY [19], TOCSY [17], and HMQC [18] spectra (see *Exper. Part*).

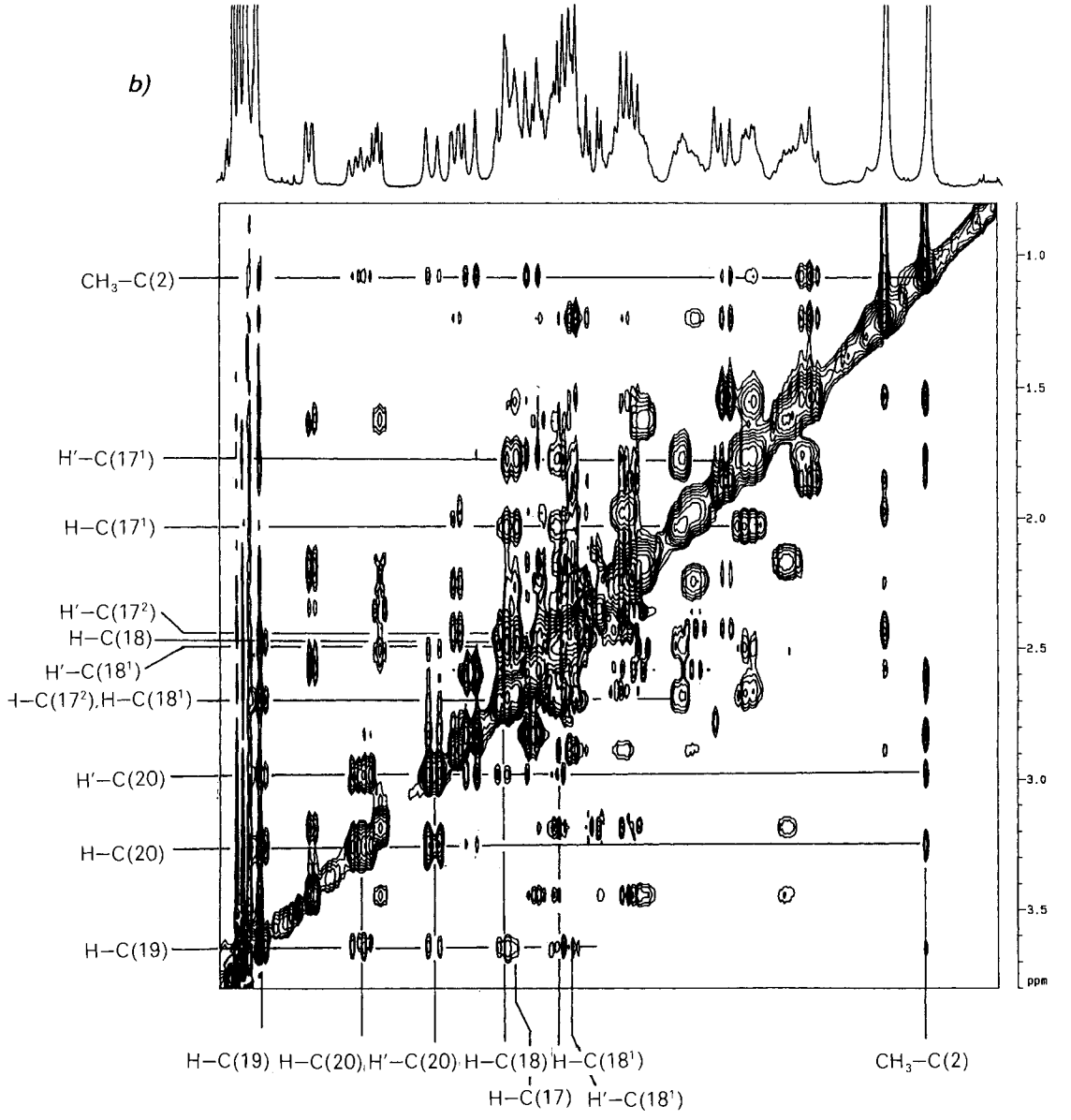

of both, **3** (*Fig. 8a*) and **5** (*Fig. 8b*)[10]) were measured at 400 MHz in $CDCl_3$ at 0° for a series of mixing times in order to follow NOE buildup and check for spin-diffusion effects.

---

[10]) The 12,13-didehydro-F430 pentamethyl ester was studied by the same NMR techniques as described here for **3** and **5**. Well resolved NOESY spectra were obtained in $CDCl_3$ at 0°. For the region of ring D, the same pattern of NOE's was observed as in **3** and **5**. In particular, the *cis*-arrangement of H–C(19) and H–C(17) followed unambiguously from a medium-intensity NOE between these protons. Since 12,13-didehydro-F430 was converted to coenzyme F430 by reduction with Zn/AcOH [3], these results independently corroborate the configurational assignment for ring D in F430.

Table 1. *^{1}H-NMR Data of F430M* (**3**) *and 12,13-Diepi-F430M* (**5**, X = ClO_4)[a])

Assignment[b])	F430M (**3**)	12,13-Diepi-F430M (**5**)	Assignment[b])	F430M (**3**)	12,13-Diepi-F430M (**5**)
H–N(6^1)	7.18	7.20	H–C(8^2)	2.58	2.58
$CONH_2$ (1 H)	6.44	6.40	H′–C(17^2)	2.50	2.47
H–C(10)	5.72	5.85	H–C(18)	2.50	2.53
$CONH_2$ (1 H)	5.68	5.46	H′–C(18^1)	2.48	2.50
H–C(4)	4.48	4.54	H′–C(8^2)	2.47	2.48
H–C(13)	3.80	3.53	H–C(7^1)	2.47	2.47
CH_3O[c])	3.71 (3 H),	3.72 (6 H),	H′–C(7^1)	2.38	2.37
	3.68 (6 H),	3.70 (3 H),	CH_2(3^2)	2.30	2.30
	3.64 (3 H),	3.68 (3 H),	H–C(13^2)	2.30	2.53
	3.62 (3 H)	3.66 (3 H)	H–C(8^1)	2.22	2.25
H–C(19)	3.53	3.68	H′–C(13^2)	2.13	2.46
H–C(20)	3.15	3.12	H–C(17^1)	2.11	2.08
H–C(12)	3.12	3.21	H′–C(8^1)	1.96	1.96
H′–C(20)	2.98	2.98	H–C(13^1)	1.90	2.12
H–C(8)	2.84	2.92	H–C(5)	1.87	1.84
H–C(2^1)	2.78	2.81	H–C(3^1)	1.79	1.78
H–C(3)	2.71	2.66	H′–C(17^1)	1.76	1.71
H–C(17)	2.70	2.70	H′–C(13^1)	1.68	1.80
H–C(12^1)	2.67[d])	2.35	H′–C(3^1)	1.60	1.60
H′–C(12^1)	2.65[d])	2.22	H′–C(5)	1.53	1.45
H–C(17^2)	2.64	2.66	CH_3–C(7)	1.20	1.22
H′–C(2^1)	2.63	2.59	CH_3–C(2)	1.11	1.09
H–C(18^1)	2.63	2.67			

[a]) 400-MHz spectra in CD_2Cl_2 at 25°. Chemical-shift values are referenced to $CDHCl_2$ (= 5.33 ppm).
[b]) The assignments are based on COSY, TOCSY, NOESY, and HMQC spectra.
[c]) Not individually assigned.
[d]) Approximate δ values. In **3**, the signals of CH_2(12^1) form the almost degenerate *AB* part of an *ABX* system.

In the NOESY spectra of F430M (**3**), cross-peaks corresponding to all NOE correlations previously established by 1D-NOE-difference spectroscopy were observed. Additionally, for the region of ring D, the spectra exhibited cross-peaks for H–C(19)/H–C(20)(medium), H–C(19)/H′–C(20)(weak), and H–C(19)/H–C(18^1)(weak) which were not detected or could not be assigned by 1D spectroscopy at 25°[11]). The signal of H–C(17) was too broad to allow observation of NOE correlations to this proton in the 2D spectrum at 0°. In the 1D-NOE-difference spectra (CD_2Cl_2, 25°), a medium-intensity NOE between H–C(19) und H–C(17) (which now could be assigned from the 2D spectra) had been observed. Accidental overlap of signals from H′–C(18^1) and H–C(18) precluded definitive assignment of their cross-peaks with H–C(19), H–C(20), and H′–C(20).

The cross-peak patterns in the 2D-NOESY spectra of 12,13-diepi-F430M (**5**, X = ClO_4) closely matched those observed for **3**. Due to the better resolution[8]) and slightly different chemical-shift values, cross-peaks for H–C(19)/H–C(17)(medium), H–C(19)/H′–C(18^1)(medium), H–C(19)/H–C(18)(weak), H′–C(20)/H–C(2^1)(medium), and H′–C(20)/H–C(18)(weak) could be assigned for **5**, in addition to those observed for **3**.

[11]) Nonequivalent CH_2 protons are designated with H and H′, respectively, with H′ resonating at higher field.

Table 2. *^{13}C-NMR Data of F430M* (**3**) *and 12,13-Diepi-F430M* (**5**, X = ClO_4)[a])

Assignment[b])	F430M (**3**)	12,13-Diepi-F430M (**5**)	Assignment[b])	F430M (**3**)	12,13-Diepi-F430M (**5**)
C(17^3)	194.6	194.4	C(17)	50.8	50.1
C(1)	188.9	187.8	C(13)	50.3	51.6
C(14)	176.9	175.7	C(7)	50.2	50.9
C(9)	176.7	174.4	C(18)	45.5	45.8
	173.6	174.2	C(12)	45.2	45.9
	173.5	173.34	C(3)	44.3	43.5
	173.4	173.26	C(7^1)	43.8	43.6
$CONH_2$	173.1	173.1	C(2^1)	42.1	42.1
$COOCH_3$	172.6	172.7	C(12^1)	39.7	38.5
		172.2	C(17^2)	38.7	38.8
	172.3	171.7	C(5)	36.1	36.1
	171.7	171.3	C(18^1)	34.7	34.5
C(11)	169.2	167.8	C(3^2)	32.8	32.7
C(15)	109.6	109.6	C(8^2)	32.6	32.1
C(10)	98.4	98.8	C(13^2)	31.7	32.5
C(6)	92.3	92.0	C(13^1)	29.8	29.1
C(4)	65.5	65.2	C(20)	28.4	28.3
C(19)	63.7	63.6	C(17^1)	25.7	25.1
C(8)	57.0	56.4	C(8^1)	22.4	22.2
C(2)	54.8	[c])	C(3^1)	20.2	20.2
	52.5	52.4	CH_3–C(2)	20.2	20.2
CH_3O	52.3 (3C), 52.0	52.3 (3C), 52.1	CH_3–C(7)	15.6	15.5

[a]) ^{1}H-Broad-band-decoupled spectra (100 MHz) in CD_2Cl_2 at 25°. Chemical-shift values are referenced to CD_2Cl_2 (= 53.84 ppm).

[b]) Assignments of all H-bearing C-atoms are based on HMQC spectra.

[c]) This signal is probably obscured by the solvent signal (53.0–54.6 ppm).

Because of the crucial dependence of the configurational assignments on the cross-peaks CH_2(20)/H–C(19), their buildup rates were compared to those of the geminal H–C(20)/H′–C(20) NOE for both, **3** and **5** (*Fig. 9*), in order to check for indirect NOE's (spin diffusion). The four curves all exhibit the shape which is characteristic for direct NOE's [20]. The ratio between the initial buildup rates of the geminal *vs.* the vicinal NOE's and between the two vicinal NOE's is similar for both **3** and **5**.

Assignment of Configuration at C(19). Taking into account that the methylene group at C(20) may have conformational flexibility and the observed spectra could be the result of rapid exchange between different conformations, two (extreme) conformations for each possible configuration (19*R* or 19*S*) are considered, *i.e.* **Ia** and **Ib**, or **IIa** and **IIb**. Proton H–C(19) is coupled to H–C(20) with J = 9 Hz, whereas the coupling constant to H′–C(20) is < 1 Hz[11]). Because of the large difference in the (possibly averaged) coupling constants, the dihedral angle H–C(19)–C(20)–H can not deviate more than *ca.* 30° from either 0 or 180° in the predominant conformation while H–C(19)–C(20)–H′ must be near 90°[12]). The CH_3 group at C(2) points to the α-side in quasi-axial direction as shown by NOE's to H_α–C(5) and H–C(3^1) [1]. In the NOESY spectra, this CH_3 group shows

[12]) In the X-ray structure of **5**, with H-atoms added in positions calculated from stereochemical considerations, these dihedral angles are 25.8° for H–C(19)–C(20)–H and 91.5° for H–C(19)–C(20)–H′.

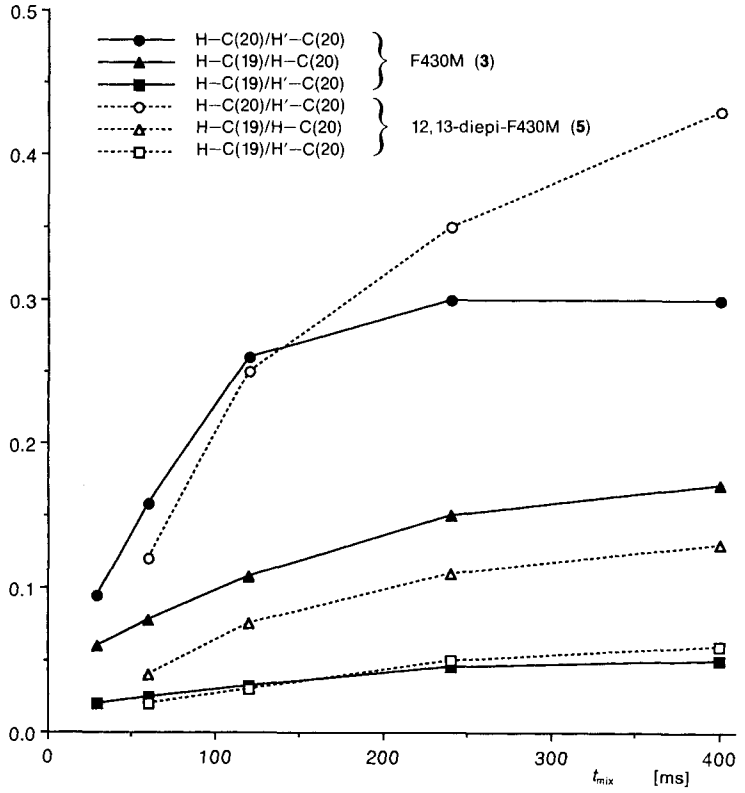

Fig. 9. *Buildup of the NOESY cross-peaks H–C(20)/H–C(19), H'–C(20)/H–C(19), and H–C(20)/H'–C(20) in F430M* (**3**) *and 12,13-diepi-F430M* (**5**). Ratio between cross-peaks and the diagonal peak at the same ω_1 value for different mixing times.

cross-peaks to both H–C(20) and H'–C(20), the former being *ca.* 4 times more intense than the latter[13]). Therefore, the major conformation must correspond to either **Ia** or **IIa**.

Based on the stronger NOE with CH_3–C(2) and $J = 9$ Hz for the coupling to H–C(19), H–C(20) can be assigned to H_α (quasi-axial) whereas H'–C(20) corresponds to H_β (quasi-equatorial). Since in **3** H–C(19) shows a NOESY cross-peak to H_α–C(20) which is *ca.* three times stronger than the one to H_β (in **5**, the ratio is *ca.* 2.4), H–C(19)

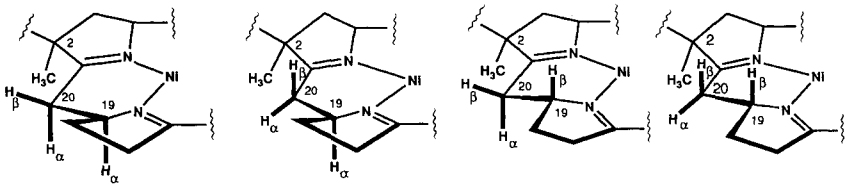

Ia (19*R*) **Ib** (19*R*) **IIa** (19*S*) **IIb** (19*S*)

[13]) From the 1D-NOE-difference spectra, these NOE's were judged to be roughly comparable [1].

must point to the α-side and the (19*R*)-configuration has to be assigned to C(19). If the configuration were (19*S*) and the predominant conformation **IIa**, the NOE observed between H–C(19) and H_α would have to be attributed to a minor conformation like **IIb** with H_α in a quasi-equatorial and H_β in a quasi-axial position. This is, however, not consistent with the observation of a weaker NOE to H_β which would be nearer to H–C(19) than H_α in both conformations.

While there are subtle differences in the coupling constants and NOE intensities, the 2D spectra of F430M (**3**) and 12,13-diepi-F430M (**5**, X = ClO_4) are very similar, and the configurational analysis leads to the same relative configurations in both compounds[9]).

Relative Configuration at C(17), C(18), and C(19). 1D-NOE's (and, in the case of **5**, a corresponding NOESY cross-peak) between H–C(19) and H–C(17) indicate that the two protons are *cis* to each other in both **3** and **5**. For **5**, cross-peaks between H–C(19) and both protons of $CH_2(18^1)$ on one hand, and between the quasi-equatorial H′–C(20) and H–C(18) on the other hand indicate that H–C(18) points to the β-side and the relation between the three protons H–C(17), H–C(18), and H–C(19) is *trans,trans*. The same cross-peaks are present in the NOESY spectra of **3**, but due to accidental overlap between H′–C(18^1) and H–C(18), they do not permit a definitive interpretation of this NOE. However, the coupling constants $J(18,19) = 9$ und $J(18,17) \approx 10$ Hz, both similar in **3** and **5**, are not consistent with a *cis,cis*-arrangement which would be the only alternative. In their recent NMR analysis of coenzyme F430 in CF_3CD_2OD, *Summers* and coworkers also deduced a *trans,trans*-relationship for H–C(17), H–C(18), and H–C(19) based on NOESY and ROESY spectra [11].

5. Conclusion. – The results described herein finally resolve the long-standing problem concerning the configuration in ring D of coenzyme F430 (**2**). The X-ray analysis of 12,13-diepi-F430M (**5**, X = Br) and the chemical correlation of its configuration in ring D with that of F430M (**3**) allowed the assignment of configuration at C(17), C(18), and C(19). NMR studies of both 12,13-diepi-F430M (**5**, X = ClO_4) and F430M (**3**) independently led to the conclusion that in both compounds, the configuration at C(19) is (19*R*) and that H–C(17) and H–C(19) are *cis* to each other. The results confirm our original assignments of the relative and absolute configuration in rings A, B, and C, but show that our previous tentative assignments for C(18) and C(19) [1] have to be reversed. *With the available evidence for the (17S,18S,19R)-configuration in ring D, the configuration of coenzyme F430 is now considered to be known for all stereogenic centers* (*cf. Formula* **2**).

In addition, the crystal-structure analysis of 12,13-diepi-F430M (**5**, X = Br) has provided the first detailed conformational picture of a molecule closely related to coenzyme F430 (**2**). Its most prominent feature is the highly ruffled, saddle-shaped deformation of the macrocycle, demonstrating that the ligand conformation of **5** is governed by the same principles which have been derived from the systematic study of synthetic hydroporphinoid low-spin Ni^{II} complexes [12a]. The structural data may serve as a basis for the conformational analysis of coenzyme F430 (**2**) and related compounds. They also provide a more solid ground for our previous discussion of the interrelation between the conformation of **2** and its reactivity at the ligand periphery and at the Ni center [3].

Experimental Part

Epimerization of Coenzyme F430 (**2**) *in* D_2O. F430 (**2**; 14 mg; *ca.* 11 μmol according to UV/VIS) [1] was dissolved in D_2O (2 ml; 99.9% D) and the soln. evaporated at 30°/20 Torr. This procedure was repeated once. The resulting residue was redissolved in D_2O (1.5 ml) and transferred to an ampoule with a vacuum-tight *Teflon* stopcock. After degassing at 0.01 Torr by three freeze/thaw cycles, the soln. was heated under Ar at 100° for 19 h. The mixture was diluted with 2.5 ml of D_2O and lyophilized. To the crude product, CD_3OD (4 ml; > 99% D) and $TsOD \cdot D_2O$ (76 mg; 0.4 mmol)[14]) were added. The resulting soln. was degassed by three freeze/thaw cycles and stirred under Ar at 40° for 4 h. The ice-cooled mixture was diluted with 15 ml of CH_2Cl_2 and extracted 3 × with aq. 0.1M $NaClO_4$. After filtration through cotton and evaporation, the yellow residue was purified by TLC ($NaClO_4$-coated silica-gel plate [1], 4 developments with CH_2Cl_2/MeOH 13:1. The main product (yellow band at R_f *ca.* 0.5) was isolated and repurified according to [1]. The resulting amorphous sample of partially deuterated 12,13-diepi-F430M ([D]-**5**, X = ClO_4; 4.5 mg, *ca.* 40%) was prepared for NMR spectroscopy as described in [1]. ^{1}H-NMR (400 MHz, CD_2Cl_2): 1.08 (*s*, CH_3–C(2)); 1.20 (*s*, CH_3–C(7)); 1.46 (*t*, *J* = 13, 1 H, H_α–C(5)); 1.5–2.75 (*ca.* 25 H); 2.81 (*d*, *J* = 17, 1 H, H–C(2^1)); 2.99 (*d*, *J* = 18, 1 H, H_β–C(20)); 3.13 (*dd*, *J* = 10, 18, *ca.* 0.6 H, H_α–C(20)); 3.55–3.64 (3 weak br. *s*, 0.2 H, $COOCD_2H$); 3.68 (*m*, 1 H, H–C(19)); 4.48 (*m*, 1 H, H–C(4)); 5.86 (*s*, 1 H, H–C(10)); 5.48, 6.23 (2 br. *s*, 1 H each, $CONH_2$); 6.87 (*s*, 1 H, NH–C(6)); comparison with the spectrum of undeuterated **5** (*cf. Table 1* and [3]): H–C(8), H–C(12), and H–C(13) are missing. ^{13}C-NMR (100 MHz, CD_2Cl_2): comparison with undeuterated **5** (*cf. Table 2*): C(12), C(13), C(8), and one of the 2 signals at 39 ppm (C(17) or C(12)) are missing; the intensity of C(20) is reduced by *ca.* 50%; all other signals are present ($\Delta\delta$ < 0.5 ppm).

X-Ray Crystal-Structure Analysis of 12,13-Diepi-F430M (**5**, X = Br). Reddish-brown crystals ($C_{47}H_{61}BrN_6NiO_{13} \cdot 0.65\ C_3H_6O_2$, mol.wt. 1104.8) were obtained from a soln. of **5** (4 mg) in 0.3 ml of AcOMe/CH_2Cl_2 10:1 upon standing at r.t. A crystal of dimensions 0.6 × 0.7 × 0.8 mm^3 was investigated using an extensively modified *Stoe* 4-circle diffractometer (MoK_α radiation, λ = 0.71069 Å, graphite monochromator) equipped with a *Nonius* cold-stream device. The crystal was immersed in a hydrocarbon oil, picked up with a glass fiber, and quickly cooled to 93(2) K (temp. recorded *ca.* 6 mm before the crystal) in the cold-stream of the low-temp. device [21].

Cell dimensions and the crystal-orientation matrix were determined by a least-squares fit to the setting angles of 36 reflections in the range 5.5° < 2θ < 13°: space group *R*3, *a* = 22.863(12), *c* = 26.686(20), *V* = 12081(3) Å^3, *Z* = 9, d_{exp} = 1.41(1) g/cm^3 (flotation method from CCl_4/hexane at 295 K), d_{calc} = 1.37 g/cm^3 (calculated with the cell constants at 93 K, for the above composition including a molecule of AcOMe with a site-occupation factor of 0.65, as obtained from the refinement).

Data were collected for a complete hemisphere of reciprocal space with 5.5° < 2θ < 50° ($-27 \leq h \leq 27$, $-27 \leq k \leq 27$, $0 \leq l \leq 31$), using an ω-scan type (scan width 1.0°), stationary background/peak/stationary background method, variable scan time, depending on the intensity observed in a fast pre-scan. The integrity of instrument and crystal was checked by periodically remeasuring three standard reflections (every 100 reflections); their intensities showed an r.m.s. fluctuation of 1.6%, and a largest deviation of any reflection from its mean value of 6%. Of the 14941 reflections observed, 10181 had $I/\sigma(I) > 1.5$, of which 3927 unique. LP corrections were applied, but no absorption correction at this point (μ = 11.7 cm^{-1}, calculated for full occupancy of the disordered AcOMe solvent molecule, see below).

Fig. 10a shows a normal probability plot [22] of *I*(*hkil*) – *I*(*ihkl*), *i.e.*, of the differences between reflections that are symmetry-equivalent in the rhombohedral space group *R*3 (but not in the triclinic space group *P*1). The slope of the plot is 1.26 and its intercept is –0.26. The merging of symmetry-equivalent reflections yielded an *R* value between symmetry-equivalent *F* quantities of *R*(sym) = 0.0119 (merging of 10181 reflections with $I/\sigma(I) > 1.5$ to yield 3927 unique reflections). The corresponding normal probability plot (for *F* values), after application of an empirical absorption and volume correction (see below), is shown in *Fig. 10b*; its slope is 1.09, with zero intercept, and *R*(sym) = 0.0098. We believe that *Fig. 10b* not only corroborates the rhombohedral symmetry, but also documents the good quality of the data.

The structure solution had previously been obtained by *Patterson* and difference *Fourier* techniques with an older data set [10]. This solution was used as a starting point. Subsequent cycles of refinement and difference *Fourier* syntheses yielded all atoms of the F430M molecule, with the exception of the terminal $COOCH_3$ C-atom of the C(18) acetate group. The disorder observed for the propionate side chain attached to C(13) and the acetate substituent at C(18) was accounted for by two conformations for each of these side chains, starting from the β-atom. Both conformations were refined independently, with the sum of their s.o.f.'s constrained to unity. Bond

[14]) Prepared from $TsOH \cdot H_2O$ (160 mg) by addition/evaporation of D_2O (2 × 0.5 ml) and drying at 0.05 Torr/r.t. for 16 h.

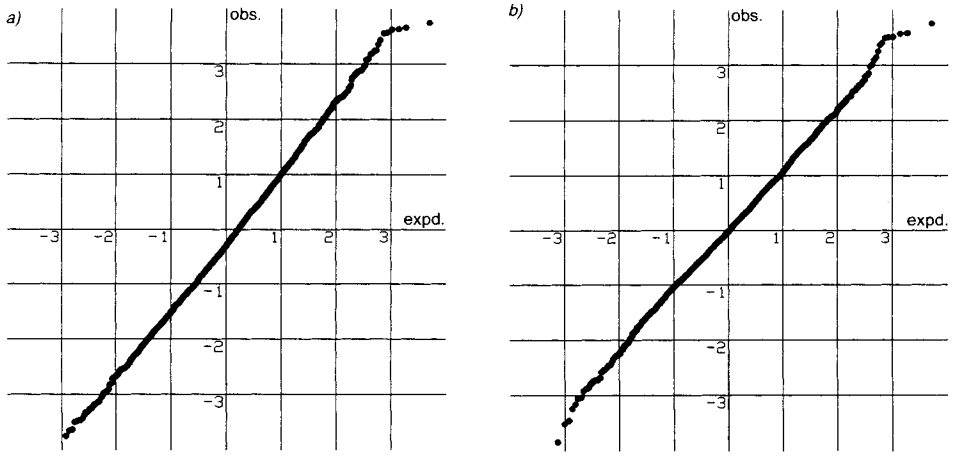

Fig. 10. *Normal probability plots for the crystal structure of* I(hkil) – I(ihkl) *for the crystal structure of* **5**. The two intensities are symmetry equivalent in $R\bar{3}$. *a*) Raw data, *b*) after an empirical absorption and volume correction.

lengths in these two side chains were constrained to configurationally reasonable values, and an isotropic a.d.p. was refined for each partial atom. At this point ($R = 0.12$), an empirical absorption, extinction, and volume correction was applied (program DIFABS [23]). Due to suspected (insufficiently corrected) extinction, 11 strong low-order reflections with large and negative ($F_{obs} - F_{calc}$) differences were excluded.

All non-H-atoms of **5** not affected by disorder were subsequently refined with anisotropic a.d.p.'s. H-Atoms whose positions are uniquely defined from configurational considerations were included in the refinement at calculated positions, with an isotropic a.d.p. allowed to refine for each of them.

Four electron-density maxima were ascribed to the disordered Br^- counter ion, and refined with anisotropic a.d.p.'s. One of these positions lies on the threefold axis; it was assumed to be fully occupied. A site-occupation factor was refined for each of the remaining three atoms. At the close of the refinement, the sum of the products of the four s.o.f.'s with their corresponding multiplicities was 0.987(21).

A partially disordered solvent molecule (AcOMe) was also observed in difference electron density maps. It was refined with isotropic a.d.p.'s and a (common) s.o.f. which converged to a value of 0.65. Its bond lengths were constrained to configurationally reasonable values. An isolated peak which we believe to originate from a second disordered solvent molecule was accounted for by refining an isotropic C-atom at this position; its isotropic a.d.p. converged to 0.11(1) $Å^2$.

The refinement, which involved 677 parameters and 3927 observations during its last cycles, converged at $R = 0.0787$ and $R_w = 0.061$ ($1/\sigma^2$ weights). To establish the absolute configuration, the final coordinates were inverted, and the refinement was continued under identical conditions. The enantiomeric structure converged at $R = 0.084$ and $R_w = 0.066$. A final difference electron density map showed positive features up to 0.8 $eÅ^{-3}$ and negative features down to 0.5 $eÅ^{-3}$. The largest positive residual electron density was observed near the terminal atoms of the (disordered) C(18) substituent. The atomic coordinates have been deposited at the *Cambridge Crystallographic Data Centre*. The computer programs used for this and the preceding structure analysis of **5** [10] are listed in [23] [24].

NMR Spectroscopy of F430M (**3**) *and 12,13-Diepi-F430M* (**5**, X = ClO_4). For 1D-NOE-difference spectroscopy, see [1a]. *Bruker AMX400* spectrometer, temperature control to 0.1 K, measured by Pt-100 thermometer inserted into the probe in place of the sample tube. Samples: **3** (15 mg; $c = 20$ mM) and **5** (12 mg; $c = 16$ mM) in 0.6 ml of CD_2Cl_2 or $CDCl_3$, degassed at a vacuum line and sealed in a 5-mm NMR tube. COSY: double-quantum-filtered phase-sensitive (TPPI) spectra; 4 K(ω_2) × 512(ω_1) data points acquired, 32 scans per FID; transformed after multiplication with a sine bell shifted by $\pi/4$ in ω_2 and a sine square function shifted by $\pi/3$ in ω_1; zero filling to give a 2 K × 1 K real × real data matrix. TOCSY: isotropic mixing with MLEV-17 ($\gamma B_2/2\pi = 9$ kHz); mixing time 80 ms, phase sensitive (TPPI); 512 FID's of 4 K data points in ω_2, 16 scans each were acquired; transformed with a sine square filter shifted by $\pi/4$ in ω_2 and $\pi/3$ in ω_1 to give a 2 K × 1 K real × real matrix. HMQC: BIRD relaxation filter (0.25 s), GARP ^{13}C-broad-band decoupling, phase sensitive (TPPI); 2 K(ω_2) × 256(ω_1) data points acquired with 32 scans per FID; transformed after multiplication with a sine square function shifted by $\pi/3$ in ω_2

and a *Gaussian* filter in ω_1 to give a 1K × 1K real × real data matrix. ROESY [16]: MLEV-17 spin lock ($\gamma B_2/2\pi = 4$ kHz), mixing time 120 ms with a 90° pulse sandwich [16c], phase sensitive (TPPI); 4 K(ω_2) × 512(ω_1) acquisition, 32 transients per FID; transformed after multiplication in both dimensions with a sine square function shifted by $\pi/2$ and zero filling to give a 2 K × 1 K real × real data matrix; baseline correction by third order polynomial fitting. NOESY: phase sensitive (TPPI) with random variation of mixing times by ± 5% for $\tau_{mix} \geq 200$ ms and 15% for $\tau_{mix} < 200$ ms; 2K(ω_2) × 256(ω_1) acquisition with 64 transients/FID; transformed after multiplication with sine square shifted by $\pi/3$ in ω_2 and $\pi/2$ in ω_1; zero filling to give a 1024(ω_2) × 512(ω_1) real × real data matrix; polynomial baseline correction in ω_2.

REFERENCES

[1] a) A. Pfaltz, B. Jaun, A. Fässler, A. Eschenmoser, R. Jaenchen, H. H. Gilles, G. Diekert, R. K. Thauer, *Helv. Chim. Acta* **1982,** *65,* 828; b) A. Fässler, A. Pfaltz, P. M. Müller, S. Farooq, C. Kratky, B. Kräutler, A. Eschenmoser, *ibid.* **1982,** *65,* 812.

[2] D. A. Livingston, A. Pfaltz, J. Schreiber, A. Eschenmoser, D. Ankel-Fuchs, J. Moll, R. Jaenchen, R. K. Thauer, *Helv. Chim. Acta* **1984,** *67,* 334.

[3] A. Pfaltz, D. A. Livingston, B. Jaun, G. Diekert, R. K. Thauer, A. Eschenmoser, *Helv. Chim. Acta* **1985,** *68,* 1338.

[4] A. Fässler, A. Kobelt, A. Pfaltz, A. Eschenmoser, C. Bladon, A. R. Battersby, R. K. Thauer, *Helv. Chim. Acta* **1985,** *68,* 2287.

[5] R. P. Gunsalus, R. S. Wolfe, *FEMS Microbiol. Lett.* **1978,** *3,* 191; G. Diekert, B. Klee, R. K. Thauer, *Arch. Microbiol.* **1980,** *124,* 103; W. B. Whitman, R. S. Wolfe, *Biochem. Biophys. Res. Commun.* **1980,** *92,* 1196.

[6] Reviews: A. Pfaltz, 'Structure and Properties of Coenzyme F430', in 'The Bioinorganic Chemistry of Nickel', Ed. J. R. Lancaster, Jr., VCH Publishers, New York, 1988, pp. 275–298; A. Pfaltz, *Chimia* **1990,** *44,* 203.

[7] P. E. Rouvière, R. S. Wolfe, *J. Biol. Chem.* **1988,** *263,* 7913.

[8] T. A. Bobik, K. D. Olson, K. M. Noll, R. S. Wolfe, *Biochem. Biophys. Res. Commun.* **1987,** *149,* 455; J. Ellermann, R. Hedderich, R. Böcher, R. K. Thauer, *Eur. J. Biochem.* **1988,** *172,* 669.

[9] B. Jaun, A. Pfaltz, *J. Chem. Soc., Chem. Commun.* **1988,** 293; B. Jaun, *Helv. Chim. Acta* **1990,** *73,* 2209; B. Jaun, 'Redox Chemistry of Coenzyme F430, the Hydrocorphinoid Nickel Complex Catalysing Methane Formation in Methanogenic Bacteria', in 'The Biological Alkylation of Heavy Elements', Eds. P. J. Craig and F. Glockling, Special Publ. No. 66, The Royal Society of Chemistry, London, 1988, pp. 20–30.

[10] W. Keller, Ch. Kratky, published in W. Keller, Dissertation, Universität Graz, 1989.

[11] H. Won, K. D. Olson, R. S. Wolfe, M. F. Summers, *J. Am. Chem. Soc.* **1990,** *112,* 2178; K. D. Olson, H. Won, R. S. Wolfe, D. R. Hare, M. F. Summers, *ibid.* **1990,** *112,* 5884.

[12] a) C. Kratky, R. Waditschatka, C. Angst, J. E. Johansen, J. C. Plaquevent, J. Schreiber, A. Eschenmoser, *Helv. Chim. Acta* **1985,** *68,* 1312; b) C. Kratky, to be published.

[13] M. Zimmer, R. H. Crabtree, *J. Am. Chem. Soc.* **1990,** *112,* 1062.

[14] D. Neuhaus, *J. Magn. Reson.* **1983,** *53,* 109.

[15] a) J. Jeener, B. H. Meier, P. Bachmann, R. R. Ernst, *J. Chem. Phys.* **1979,** *71,* 4546; b) S. Macura, R. R. Ernst, *Mol. Phys.* **1980,** *41,* 95.

[16] a) A. A. Bothner-By, R. L. Stephens, J. Lee, C. D. Warren, R. W. Jeanloz, *J. Am. Chem. Soc.* **1984,** *106,* 811; b) A. Bax, D. G. Davis, *J. Magn. Reson.* **1985,** *63,* 207; c) C. Griesinger, R. R. Ernst, *ibid.* **1987,** *75,* 261.

[17] a) L. Braunschweiler, R. R. Ernst, *J. Magn. Reson.* **1983,** *53,* 521; b) A. Bax, D. G. Davis, *ibid.* **1985,** *65,* 355.

[18] a) L. Müller, *J. Am. Chem. Soc.* **1979,** *101,* 4481; b) A. Bax, S. Subramanian, *J. Magn. Reson.* **1986,** *67,* 565.

[19] M. Rance, O. W. Sørensen, G. Bodenhausen, G. Wagner, R. R. Ernst, K. Wüthrich, *Biochem. Biophys. Res. Commun.* **1983,** *117,* 479.

[20] A. Kumar, G. Wagner, R. R. Ernst, K. Wüthrich, *J. Am. Chem. Soc.* **1981,** *103,* 3654.

[21] H. Hope, *ACS Symp. Ser.* **1987,** *357,* 257; H. Hope, *Acta Crystallogr., Sect. B* **1988,** *44,* 22; H. Hope, F. Frolow, K. von Böhlen, I. Makowski, C. Kratky, Y. Halfon, H. Danz, P. Webster, K. S. Bartels, H. G. Wittman, A. Yonath, *ibid.* **1989,** *45,* 190.

[22] S. C. Abrahams, E. T. Keve, *Acta Crystallogr., Sect. A* **1971,** *27,* 157.

[23] N. Walker, D. Stuart, *Acta Crystallogr., Sect. A* **1983,** *39,* 158.

[24] G. M. Sheldrick, 'SHELX76', a Program for Crystal Structure Determination, Univ. of Cambridge, England, 1976; S. Motherwell, 'PLUTO, a Program for Plotting Molecular and Crystal Structures', Cambridge Crystallographic Data Centre, England, 1976; G. M. Sheldrick, 'SHELXS-86', Universität Göttingen, 1986; C. K. Johnson, 'ORTEP, Report ORNL 5138', Oak Ridge National Laboratory, Oak Ridge, Tennessee, USA, 1976.